TABLE I. Comparison of results for Fe and Zn. N_μ=number of stopped muons; N_γ=total number of γ rays between 4 and 10 Mev; ϵ=total detection efficiency; Y=γ-ray yield per capture muon.

Element	N_μ	N_γ	ϵ	Y
Fe	9.0×10^5	2997	1.21×10^{-2}	0.302 ± 0.005
Zn	1.8×10^5	638	1.34×10^{-2}	0.285 ± 0.010

capture events. Since the neutron multiplicity is $\cong 1$ per muon capture, even a small probability of a neutron's being captured in the NaI crystal and producing γ rays in the 4–10 Mev region could produce an appreciable background. For this reason, one must regard the yield as an upper limit.

However, if one assumes that this yield is purely capture γ rays which might be detected in an electron

telescope of the type used by Yovanovitch,[1] and a detection efficiency of 1% for such γ rays is assumed (again an upper limit), then the maximum possible error that could be caused by such a spurious process in the bound muon decay rate for iron would be $\cong 3\%$. Furthermore the same effect would occur for zinc, where there is no decay-rate anomaly.

We conclude that the mechanism suggest by Chilton cannot be the cause of the decay-rate anomaly.

Since completing this work, we have learned that a CERN group (G. Culligan, D. Harting, N. H. Lipman, and G. Tibell) have searched again for the decay-rate anomaly in iron, but have failed to find it.

ACKNOWLEDGMENT

C¹²(p,pn)C¹¹ Cross Section at 28 Gev*

J. B. CUMMING, G. FRIEDLANDER, AND S. KATCOFF

Chemistry Department, Brookhaven National Laboratory, Upton, New York

(Received November 7, 1961)

The $C^{12}(p,pn)C^{11}$ cross section has been measured in the 28-Gev diffraction scattered proton beam of the Brookhaven AGS. Proton fluxes were determined using nuclear emulsions and the C^{11} activity induced in plastic scintillators was measured by internal scintillation counting. The cross section at 28 Gev is 25.9 ± 1.2 mb, not significantly different from the values at 2 and 3 Gev.

INTRODUCTION

THE cross sections of the $C^{12}(p,pn)C^{11}$ and $Al^{27}(p,3pn)Na^{24}$ reactions have been used as the primary standards for a large number of radiochemical and physical measurements of cross sections for high-energy-proton interactions. In the Gev region, only the $C^{12}(p,pn)C^{11}$ cross section has been measured absolutely.[1,2] The present paper reports the results of measurements of this cross section[3] at 28 Gev in the external diffracted beam of the Brookhaven AGS. Nuclear emulsions were used to measure the proton fluxes incident on plastic scintillator targets. The 20.4

min C^{11} activity produced in the plastic was measured by internal scintillation counting.

EXPERIMENTAL ARRANGEMENT

The beam was ejected from the machine by diffraction scattering in a 1.5-mm aluminum target. It emerged through a collimator in the main shielding wall and was then magnetically analyzed. There was no collimation after the magnetic analysis. This experiment was performed ~ 65 ft beyond the analyzing magnet; at this point the full-energy protons were ~ 29 in. from the undeflected beam line. Emulsion studies[4] in this region had shown a peak at the predicted location for full-energy protons and a tail of degraded charged particles. This peak accounted for $\sim \frac{1}{3}$ of the intensity of the entire beam emerging from the collimator.[4] Exposure of emulsions and plastic scintillators at $\frac{1}{2}$ degree below the main beam (8 in.) indicated that the background flux both of minimum-ionizing particles and of C^{11}-producing radiations was considerably less than 1% of the main beam. Thus the number of

* Research performed under the auspices of the U. S. Atomic Energy Commission.

[1] J. B. Cumming, G. Friedlander, and C. E. Swartz, Phys. Rev. 111, 1386 (1958).

[2] N. Horwitz and J. J. Murray, Phys. Rev. 117, 1361 (1960).

[3] In this paper the small but unknown contribution of C^{13} (natural abundance 1.1%) to C^{11} production is ignored, and the cross section for the formation of C^{11} in proton irradiation of normal isotopic carbon is taken to be the $C^{12}(p,pn)C^{11}$ cross section. The notation $C^{12}(p,pn)C^{11}$ does not imply the emission of a proton and neutron, but is meant to include any other mechanism for C^{11} formation, such as deuteron emission or processes involving pions, etc.

[4] J. Hornbostel (unpublished data).

neutral particles within the analyzed beam is considered to be negligible.

Several experimental arrays of scintillators and Ilford G-5 emulsions were exposed in the analyzed diffracted beam. These are shown in Fig. 1 and will be discussed in detail below. Arrangement A was used for preliminary cross section measurements and to study the emulsion techniques used for flux measurements. Final cross section measurements were made in arrangement B. Geometry C was used only to study the flux measuring technique, and geometry D was used to measure the effects of secondary particles in producing C^{11}.

BEAM INTENSITY MEASUREMENTS

In the present experiment, the number of protons incident on plastic scintillators was measured by counting tracks in Ilford G-5 emulsions. The final cross sections were determined using the geometry B of Fig. 1. Here the beam passes first through a 2×3 in., $100\ \mu$ emulsion arranged perpendicular to the beam direction, then through a $\frac{1}{8}$-in.-thick $1\frac{1}{2}$-in.-diameter plastic scintillator. In one experiment a second emulsion was placed behind the scintillator. This perpendicular plate orientation has been used by Horwitz and Murray[2] in cross-section measurements at 3, 4.5, and 6 Gev and is reported suitable for the measurement of intensities up to 2×10^6 protons/cm^2.

The perpendicular plate technique ("plunging tracks") was compared with a parallel plate orientation ("flat tracks") at beam intensities up to 2×10^5 protons/cm^2 in geometries A and C of Fig. 1. In these geometries a crossed array of 1-in.$\times$3-in., $400\ \mu$, G-5 emulsions was irradiated behind the perpendicular plate so that the proton tracks were parallel to the emulsion surface. The flat tracks have the advantage that substantial lengths of path are available and angular distributions

FIG. 1. Various experimental arrangements used for $C^{12}(p,pn)C^{11}$ cross-section measurements.

TABLE I. Comparison of flat track and plunging track counting.

Experimental arrangement	Protons/cm^2 ($\times10^{-5}$)	
	Flat tracks	Plunging tracks
A	1.90 ± 0.04	1.88 ± 0.04
C	$1.09_5 \pm 0.01_9$	$1.05_4 \pm 0.02_0$

are readily measured. The scanning criterion for true beam tracks was that they lie within $\pm2°$ of the beam direction. If a single plate were exposed to the beam, essentially all tracks would be included in this range.[4] However, when a substantial mass of scintillator was located ahead of the emulsions as in geometry A of Fig. 1, $\sim15\%$ of the tracks fell in the range $1°$ to $10°$. With the scintillator removed as in geometry C of Fig. 1 the number of off-beam tracks having projected angles $1°$ to $10°$ was only $\sim3\%$; presumably these tracks are due to secondary particles produced by interactions in the perpendicular emulsion.

The mean fluxes incident on a $1\frac{1}{2}$-in.-diameter area of the emulsion stacks as measured by the plunging and flat track counts are compared in Table I. The observed numbers of flat tracks were reduced by 1% ao correct for secondary particles originating in the perpendicular emulsion and lying within $2°$ of the beam direction. The results of the two methods agree within the sum of the standard deviations based on the number of tracks counted. The agreement is considered quite satisfactory in view of possible small systematic errors in measuring the emulsion thickness (flat track plates) and in measuring the reticle area (plunging track plates). An area of one of the parallel plates was also scanned by a completely independent group[4] and the agreement between their result and our scan was well within the statistical uncertainty of 2%. We believe that the perpendicular track method for beam intensity measurement is as reliable and at least as convenient as the flat track method. Furthermore, intensity measurements can be made up to about 2×10^6 particles per cm^2 by counting the plunging tracks, but are limited to about 2×10^5 per cm^2 with the flat tracks.

For the final cross-section measurements, tracks were counted in nine areas of the front emulsion along vertical and horizontal diameters of the scintillators. Results for a typical plate are shown in Fig. 2. Fluxes at all nine points are within 10% of the mean value and no significant gradients are observed within the errors. The absence of sharp gradients reduces the need for extremely precise lineup of emulsions and scintillators. As a check on scanning efficiency, tracks in a number of areas were independently counted by each of two scanners. Their counts agreed within 1% and when the individual fields of view where discrepancies occurred were examined, the discrepancies could generally be resolved, e.g., a given track at the edge of a
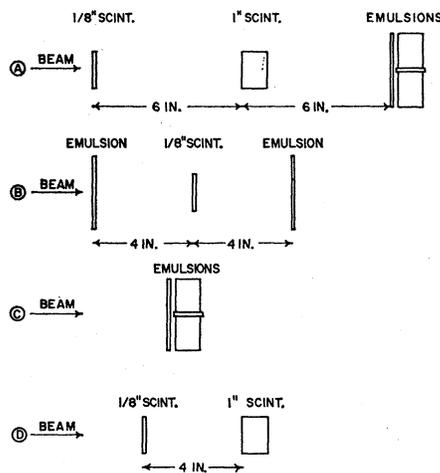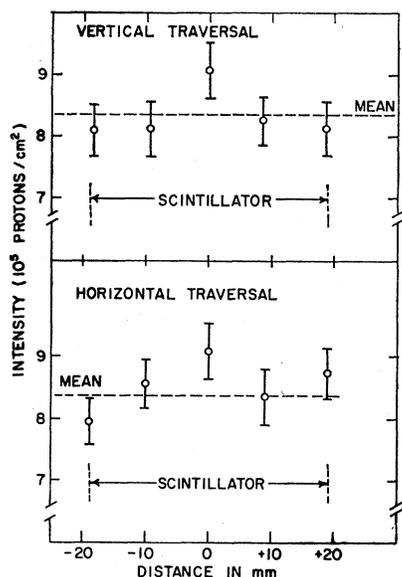
FIG. 2. Typical distribution of proton beam intensity along vertical and horizontal diameters of a scintillator target.

field had been included by one scanner but not by the other.

ACTIVITY MEASUREMENTS AND RESULTS

Plastic scintillators were irradiated in the diffracted beam for periods up to 20 min depending on the flux desired. These scintillators were fabricated from the same material as was used in previous measurements.[1,5] The integrated internal beam intensity was recorded at 2-min intervals during the irradiations to allow corrections to be made for temporal variation of the beam intensity. It had been demonstrated that the ratio of external to internal beams was essentially constant on a given day despite large longer-term variations.

The scintillators were mounted directly on Dumont 6292 or RCA 6342A photomultipliers and activity

measurements started $\sim$10 min after the end of the irradiation. The counting procedure was the same as described by Cumming and Hoffmann[5] and utilized anticoincidence techniques to reduce the counter backgrounds. Measurements were continued for several C^{11} half-lives, the discriminator settings were then calibrated with a Cs^{137} conversion electron source, and finally additional background measurements were made. Each decay curve was analyzed by a least-squares-fitting program[6] into a 20.4-min component and a background. Except for one of the preliminary runs, the computer analysis indicated that the decay curves were consistent with the presence of C^{11} and a background which agreed with measurements before and well after the irradiation.

Counting efficiencies for C^{11} in the 1-in.-thick scintillators were taken from the published data.[5] The efficiency for the $\frac{1}{8}$-in. scintillators as a function of discriminator setting was determined by ($\beta^+ - 511$ kev γ ray) coincidence measurements. For a 50 kev discriminator setting, the $\frac{1}{8}$-in. scintillator had a 94.5% counting efficiency compared to a 97.5% efficiency for the 1-in. scintillator. It has been shown[7,8] that active gas loss from the $\frac{1}{8}$-in.-thick scintillators is not significant.

From the counting data and flux measurements a cross section was calculated for each run using Eq. (1). Here D^0 is the C^{11} disintegration rate per minute at the end of an irradiation time Δt in minutes, n is the total number of carbon atoms in the scintillator and I is the mean number of protons per cm^2 as determined from the emulsions.

$$\sigma = D^0 \Delta t / f_s n I. \qquad (1)$$

The factor f_s corrects D^0 to that rate which would have been obtained from an infinitely long irradiation in a beam of mean intensity $I/\Delta t$. In the present measurements, f_s as calculated from the temporal variation of the internal beam of the AGS never differed by more than 2% from the saturation correction calculated for a uniform intensity.

TABLE II. Experimental data.

Irradiation[a]	Length of irradiation Δt, min	Protons/cm² $I \times 10^{-5}$	C^{11} disintegrations per min D^0	Saturation correction f_s	C atoms in target $n \times 10^{-23}$
A-1	13	1.89±0.03[b]	201 ± 7	0.354	13.92
A-2	{ 20	6.79±0.13[b]	74 ± 4	0.489	1.654
	{ 20	6.79±0.13[b]	641 ±17	0.489	13.95
B-1	13.6	6.52±0.09	80.2± 2.6*	0.369	1.654
B-2	12	8.36±0.13	98.0± 4.5	0.335	1.631
B-3	20	13.36±0.18	149.6± 3.6	0.496	1.654

[a] See Fig. 1.
[b] These values have been raised by 3.6% to correct for attenuation of the proton beam by the scintillators and lowered by 3% to correct for secondary particles formed in the scintillators which were included within the acceptance criteria of the scanning.

[5] J. B. Cumming and R. Hoffmann, Rev. Sci. Instr. 29, 1104 (1958).
[6] J. B. Cumming (unpublished).
[7] H. Fuchs and K. H. Lindenberger, Nuclear Instr. and Methods 7, 219 (1960).
[8] J. B. Cumming, A. M. Poskanzer, and J. Hudis, Phys. Rev. Letters 6, 484 (1961).

TABLE III. Results of cross-section measurements.

Experimental[a] arrangement	Cross section in mb
A-1	24.6±1.2[b]
A-2	26.6±1.6, 23.8±1.0[b,c]
A-Mean	25.2±1.0
B-1	26.3±1.0
B-2	24.7±1.3
B-3	26.1±0.8
B-Mean	25.9±0.6

[a] See Fig. 1.
[b] Result from 1-in.-thick target.
[c] Sample showed abnormal decay. This result not included in average.

The data of these experiments are presented in Table II and the cross sections computed from them are given in Table III. In the computation of the cross sections, various corrections have been applied to the disintegration rates shown in Table II to correct for production of C^{11} by secondary particles. For the 1-in.-thick target in run A-2 the rate was divided by 1.143 ±0.020. This is the mean value of two comparisons of the C^{11} production rate in 1-in. and $\frac{1}{8}$-in. scintillators (geometry D of Fig. 1). D^0 for the 1 in. target of run A-1 was divided by a smaller factor (1.12±0.02) since no $\frac{1}{8}$-in. scintillator was present in this case. In addition, all of the disintegration rates have been lowered by 2% to correct for the residual secondary effect in the $\frac{1}{8}$-in.-thick targets. A lower limit for this internal secondary effect can be set at ~1.5% by assuming the effect is linear with target thickness (i.e., by assuming all the secondary particles which produce C^{11} are strongly collimated forward). A somewhat higher value has been used to include the effect of the more isotropic secondaries.

Since in the final measurements (B-1, B-2, and B-3) the emulsions were ahead of the scintillators the observed C^{11} disintegration rates were lowered by an additional 2%. Due to the 4-in. separation, isotropic secondaries formed in the emulsion contribute little to C^{11} production in the scintillator. From the number of off-beam tracks observed in geometry A a lower limit of ~1.4% may be inferred for the production of C^{11} in the scintillator by charged particle secondaries from the emulsion in geometry B. The 2% correction which was used includes an estimate of the additional effect

TABLE IV. Estimates of systematic errors.

Source	Magnitude
C^{11} absolute counting	±2%
Secondary corrections	±2%
Scanning	
Efficiency	±1%
Reticle area	±2%
Track selection criterion	±2%
Rms addition	4.1%

TABLE V. Comparison with other data.

Proton energy (Gev)	Cross section (mb)	References
2.0	26.2±0.9	1
3.0	26.8±1.0	1
3.0	29.5±1.6	2
4.5	27.4±1.7	2
6.0	29.5±1.6	2
28	25.9±1.2	present work

due to neutrons which would not have been observed in the emulsions. This correction is also consistent with the observation that for geometry B the charged particle intensity measured in the second emulsion was (2.6±2.1)% greater than that in the upstream emulsion.

The standard deviations on the individual values in Table III are the root mean square combination of the standard deviations of the proton track counts, the C^{11} counting, and a 1% uncertainty in the counting efficiency. There is no indication that the measured cross sections show greater fluctuations than those predicted from these sources.

The accuracy of the mean cross section will depend on a number of possible systematic errors. These are listed in Table IV with estimates of their magnitude which have been conservatively chosen to be as large as reasonably possible. Their root mean square combination is 4.1%. When this is combined with the statistical error on the mean cross section of the B series in Table III, a value of 25.9±1.2 mb is obtained for the $C^{12}(p,pn)C^{11}$ cross section at 28 Gev. Cross sections for the $C^{12}(p,pn)C^{11}$ reaction in the Gev region are compared in Table V. The published results of Cumming et al.[1] have been increased by 0.8% to account for the gas loss[7,8] from their $\frac{1}{32}$-in. targets. Those of Horwitz and Murray[2] have been decreased by 1.1% to place them on a per-carbon-nucleus rather than per-C^{12}-nucleus[3] basis. Although the cross section at 28 Gev is slightly lower than that in the 2 to 6 Gev region, the decrease is not established with any certainty. The BNL data alone would be consistent with an energy-independent value of 26.3±1.5 mb from 2 to 30 Gev.

ACKNOWLEDGMENTS